Electrical probing of a steel rough interface under shear stress

N. Foy, E. Chevallier, H. Zerari, D. Zehouani, D. Favry

Version of Record: https://www.sciencedirect.com/science/article/pii/S0301679X20302693
Manuscript_213768e8dc52df0a8e2a3ad7825aacc9

ELECTRICAL PROBING OF A STEEL ROUGH INTERFACE UNDER SHEAR STRESS

N. Foy [a], E. Chevallier [a,*], H. Zerari [b], D. Zehouani [b] and D. Favry [b]

*eddy.chevallier@u-picardie.fr

[a] Laboratoire "Physique des Systèmes Complexes" (P.S.C. – E.A. 4663),
Université de Picardie Jules Verne, 33 rue Saint Leu, 80039 Amiens, France

[b] Département de Physique, UFR des Sciences,
Université de Picardie Jules Verne, 33 rue Saint Leu, 80039 Amiens, France

KEYWORDS

Experiments in tribology, Physics of friction, Contact and adhesion, Electrical contact resistance.

ABSTRACT

We present in this work the experimental results of shear stress applied to a rough metallic interface. This interface was test using a weak DC current, measures of the voltage evolution were done on each end of the system while an increasing shear stress was applied. From these measurements we deduce the evolution of the interface electrical resistance to attempt to highlight the contact area evolution. Results show that the interface resistance follows a non-monotonic behavior: it first increases to a maximum and then decreases until the contact breaks. The evolution of the interface resistance is related to the evolution of the contact area, the non-monotonic behavior is interpreted as different deformation regimes in the spots of contact.

1. INTRODUCTION

The contact between two rough surfaces is occurs in tiny contact spots [1] where their number, distribution, shape or size – i.e. their geometrical properties – depends on the roughness, the nature of materials, and the stress applied on the contact interface. A direct assessment of relevant parameters acting on the contact zone is difficult because of its discrete nature, so that real contact consists in a distribution of individual N micro-junctions, each one with its own surface S_k (k = 1, 2, …, N) leading to a total area A_r ($A_r = \Sigma S_k$) much smaller than the apparent contact area [2-4]. Actually, A_r follows two major behaviors: (i) it is proportional to the applied normal load [2, 5-11], and (ii) it logarithmically increases with time – as known as geometric aging or creep – [5, 12, 13].

To probe properly the interface and find relevant criteria of any influences from undergone stresses, the measurement of any appropriate physical quantities sensitive to the mechanical state is required. The measurement of electrical – or thermal – resistance corresponds perfectly to the requirements since it derives from the mechanical conditions imposed on the interface. The behavior of the interface resistance versus an applied normal stress is a well-known effect [9, 14-20]. So, it is therefore legitimate to assume that the interface resistance have also its own dependence versus an applied shear stress.

In [21] Courtney-Pratt and Eisner made an experimental study about the mechanical evolution of a spherically ended cone, bearing on a plane and undergoing a tangential force. In their study electrical measurements were made to probe the mechanical evolution of the sphere/plan contact between two polished metals of the same kind. Thus, they showed that the contact conductance seems to be proportional to the square of the shear force, for

polished platinum and steel. Due to the presence of an oxide layer, the model describing the behavior of noble metals did not make possible to correctly describe the behavior of steel.

The present paper appears as a complement on the electrical aspect of the study made in [21]. Using cylindrical polished steel samples, we focus on the influence of shear stress on the interfacial electrical resistance in order to understand the mechanical behavior of this contact interface. The experimental protocol and samples preparation were specially made in order to understand and focus on the mechanical behavior of multi-contact interfaces. Thus, emerging a behavior law between real contact area and shear stress for metallic interfaces would directly affect the slipping properties of rough contact and so, the way we use and understand tribological models.

2. MATERIAL AND METHODS

2.1 Apparatus

To study the contact interface, we use a pair of hand polished cylindrical samples made of steel (ISO683-1 C45 / AISI-SAE 1045) which were placed in a dry frictional contact arrangement in which a DC current flows (fig. 1). The applied current arrives and leaves from a small zone behind each of the samples where a wire was fixed by a silver conductive paint. Samples were sized to have a homogeneous current distribution in the bulk (fig. 2) to ensure that only the contact spots influence electrically the measure. The voltage at each end of the set was then measured during the increasing of the shear stress. The electrical probing was done by the “4 points” method using a Keithley SourceMeter 2611A wired to a computer to acquire the data.

As shown on figure 1, the lower cylinder was adhered to the table and the upper one was driven horizontally through a wire attached in the plane of the contact interface. The normal load W was applied using labelled masses and the tangential force (shear stress) F_τ is applied through a pulley by an increasing mass $m(t)$ piloted by a sandglass which delivers 6.36E-3 N/s. A sandglass was use here because of its very regular flow, which ensures a reliable application of shear on the system.

2.2 Samples preparation

Our samples were manually prepared using sandpaper to abrade the surface, then to polish them, and to finish with a 500-mesh sandpaper. For each measurement, the concerned surfaces were systematically finished and degreased with acetone before being in contact.

To know the initial surface state of the samples, a map profilometry was made with a “DektakXT Stylus Profiler” from Brucker with a 2µm stylus at 3mg of load; also EDX measures were made with a “Quanta 200 FEG scanning electron microscope” from FEI Company. The first analysis shows the overall shape of the contacting surfaces and their roughness while the second one the chemical composition of the material. The figure 3a, shows an example of a typical profile of the surface, 3b a typical map and 4 an example of an EDX spectra with the percentage content of elements in the surface.

Since our samples were manually prepared, the contact surface presents a curvature which can be fitted by a sphere (fig.3a) and so, the contact between our samples is a kind of sphere/sphere contact, where the spheres have a very large radius (~4m). From the mechanical parameters we can estimate, using the Hertz’s model, the contact zone around 0.15mm² under a normal load of 1N.

2.3 Protocol

Right after the initial contact, the following specific protocol is applied:

- [0 to 180s]: interface relaxes (creep phenomenon [5, 13, 16, 22]).
- [180s to 210s]: an increasing current is applied from 0 to 1.5A.
- [210s to 240s]: the current decreases from 1.5A to 0.25A.
- [240s to 300s]: the current is maintained to its probing value 0.25A.
- [300s to contact break-up] shear and voltage measurements begin.

The increasing/decreasing current permits to ensure the creation of contact spots, to discard thermal influences, to break a possible oxide layer, and mainly to discard Branly effect [16, 22, 23]. This last effect, actually not well understood, consists mainly of a transition to a more conductive state usually related to micro-contacts nucleation. This phenomenon, mainly observed in granular media, is also observed in contact interfaces when a DC current is directly applied, leading to a significant drop of the electrical resistance by several orders of magnitude.

To ensure a good statistics of measurements, we repeat each measurement at least five times, keeping carefully the same experimental conditions. Also, to ensure the non-appearance of an oxide layer, all measurements were done one after the other and less than five minutes after polishing and cleaning the samples.

3. RESULTS

For different normal loads W, we determine the evolution of the interface resistance R vs. shear stress F_τ (R was directly get from the voltage divided by the applied constant current value). In all experiments the interface resistance, first increases with increasing shear to reach a maximum and then decreases until the contact breaks. Figure 5 focuses on the resistance evolution of a contact undergoing a normal load around 1N and highlights the gap ΔR of resistance between the initial value R_0 (at F_τ = 0) and the maximum reached one R_{max} ($\Delta R = R_{max} - R_0$).

The existence of this gap, being reproducible, raises questions about the mechanical behavior of the contact interface. Thus, to compare each measurement, we plotted the evolution of R/R_0 vs. F_τ/W ($=\mu_S$) on the figure 6. In each case, the maximum is reached at a value close to the half of the static friction coefficient ($\mu_s \approx 0.38$), which is determined from the linear fitting on the figure 7.

The normal load has a clear effect on the top of the maximum in each measurement. To highlight its behavior we plot on figure 8 the evolution of $\Delta R/R_0$ vs. W. If we exclude the first point, we can fit the data by a power law "$y = ax^b$" where a = 1.339 and b = -1.984. The curve "$y = 4/(3x^2)$" has been added to estimate the proximity of the fit. This result leads to conclude that the normal load gradually erases the observed bump from the increment of the interface resistance by following a behavior close to the one from equation 01.

$$\frac{\Delta R}{R_0} \approx \frac{4}{3} \cdot \frac{1}{W^2} \qquad \text{(eq. 01)}$$

The decrement of the interface resistance seems to be also influenced by the normal load: the strongest the normal load, the faster the resistance decreases. If some curves remain

smooth enough to be fitted, others presents breaks – i.e. signatures of micro-displacements – making uneasy the study of this part of the behavior.

From the Holm's model describing the contact resistance R_H (eq. 02), and assuming that the contact is resume in one spot, we can deduce an associate circular area, of radius a_H, for this one (eq. 03). Note that ρ designates the resistivity of the considered material.

$$R_H = \frac{\rho}{2a_H} \quad \text{(eq. 02)}$$

$$S = \pi a_H^2 = \pi \left(\frac{\rho}{2R_H}\right)^2 \quad \text{(eq. 03)}$$

Using the same reasoning as for the resistance, we computed from eq. 03 the estimated values of $\Delta S/S_0$ and then plotted those vs. W on figure 9. For 1.5N of normal load, the gap between the initial assumed contact area and the minimum reached is about a drop of 60%. It would mean that a half of the initial contact area is lost by the shear effect.

4. DISCUSSION

In [21] the study of a steel interface was made under a normal load of 920 g wt (~10N) which is much bigger than the normal load we use. Their interpretation of the increasing conductance lies in the break of an oxide layer even if it have sense for normal load of around 10N, it does not explains why and how the conductance decreases before it increases for lower normal loads. A comparison between the results from [21] (fig. 10) and the present work (fig. 11) can possibly give a first element of answer. In both cases, the evolution of the static friction coefficient with the conductance is represented. The shape of our results is much closer to the shape of the results of the lubricated interface from [21]. Thus, the lubricant seems to emphasize an already present phenomenon which seems to not be fully related to an oxide layer break.

At the onset of slipping, old micro-junctions are replaced by smaller new ones [24]: slip inception is accompanied by a drop of real contact area [5, 12, 25, 26]. This effect is often considered to be the origin of the difference between static and dynamic friction forces [13]. For an elastomer, i.e. an elastic medium, the contact interface decreases with the shear stress due to the narrowing of the contact spots area [25-29]. In the case of the present study, the interpretation of the increasing interface conductance just as an increasing of the contact area vs. shear stress goes against those previous assertions. Metals are mainly plastic media (and it is clearly showed in [21]) but they still have an elastic behavior for weak shear stresses. This is why for a weak shear stress the mechanical behavior of the interface can be more complex than it is.

Thus, our interpretation is summarized as follow: first the contact spots react elastically to the shear stress and their area decreases (R increases), then the contact spots begin to react plastically and their area increases (R decreases). During the shearing of the interface, some contact spots break but the interface area continues to evolve until the shear stress is strong enough to surpass the adhesion force between the contact spots. The normal load assists the deformation of the contact spots, accessing them more rapidly to a plastic behavior. This explains why the measured electrical resistance gap ΔR decreases with the normal load W. In the lubricated case of [21] the lubricant, which fills the porosities due to the

roughness, creates a thickness which reduces the interpenetration of opposite surfaces, and so reduces the contact area. The lubricant acts against the normal load and so, the behavior of the interface looks like the behavior for weak normal load.

The evolution of ΔS (or ΔR) with W were well fitted as for the exception of the first point. This point is excluded to find the best fit for a maximum of data points. The relevance of its exclusion remains in coherence with the current models about the effect of the normal load [1]. However, between 1N and 1.5N, it seems that the gap is able to increase due to a complex coupling between normal and tangential stresses occurring in the contact. A future experimental campaign for weak normal loads would give answers about this hypothesis.

5. CONCLUSIONS

As prove a series of experimental peer-reviewed studies over recent decades, contact properties of multi-contact interfaces are not fully understood especially for shear stress responses. For instance, smooth metallic sphere/plane contact typically grow as shear stress increases [2, 22, 30], unlike in smooth elastomer-based sphere/plan contact [26, 31-34] where it decreases. It is therefore relevant to assume from our results that the evolution of the contact area with shear is more complex than it appears in the previous cited situations.

In the present study we highlighted a particular behavior of the mechanical response of the interface to shear stress using an electrical probing. This method has proved its effectiveness through some patents [35-37] and showed its ability to monitor the contact interface. Thus, we showed through its electrical response, the mechanical evolution of a metallic rough interface. This evolution follows a non-monotonic behavior and seems to show the distinction between two deformation regimes. Such a behavior would directly affect the understanding of the mechanical properties of contacting rough interface, the way we use current contact and friction models, and the physical meaning of the parameters of some friction law.

Note that we used only a DC current to probe the interface. So, because of the complexity of the physical situation, extend investigations based on the impedance response, i.e. impedance spectroscopy, would be an important step for a better understanding of the contact area evolution.

ACKNOWLEDGMENTS

Thanks a lot to the Physics Department at the University of Picardie Jules Verne. Thanks to Clément Puille from the LPMC for the map gotten by the DektakXT Stylus Profiler. Thanks to Arash Jamali from the electron microscopy platform “Hub de l’énergie” for the EDX analysis. Thanks to Julien Scheibert from the LTDS for discussions. Thanks to Tania B. Garcia Ramos from the LPMC for her time on the English corrections.

REFERENCES

[1] Greenwood JA, Williamson JBP. Contact of nominally flat surfaces. Proceedings of the Royal Society of London 295. Series A. Math. and Phys. Sciences (1966)

[2] Bowden FP, Tabor D. The Friction and Lubrication of Solids. Oxford University Press, Oxford (1964)

[3] Ovcharenko A, Halperin G, Etsion I. In situ and real-time optical investigation of junction growth in spherical elastic–plastic contact. Wear 264, 1043–1050 (2008)

[4] Krick BA, Vail JR, Persson BNJ, Sawyer WG. Optical in situ micro tribometer for analysis of real contact area for contact mechanics, adhesion, and sliding experiments. Tribol. Lett. 45, 185–194 (2012)

[5] Dieterich JH, Kilgore BD. Direct observation of frictional contacts: New insights for state-dependent properties. Pure Appl. Geophys. 143, 283–302 (1994)

[6] Rubinstein SM, Cohen G, Fineberg J. Detachment fronts and the onset of dynamic friction. Nature 430, 1005–1009 (2004)

[7] Yashima S, Romero V, Wandersman E, Frétigny C, Chaudhury MK, Chateauminois A, Prevost AM. Normal contact and friction of rubber with model randomly rough surfaces. Soft Matter 11, 871–881 (2015)

[8] Archard JF. Elastic deformation and the laws of friction. Proc. Roy. Soc. London A 243, 190–205 (1957)

[9] Persson BNJ, Albohr O, Tartaglino U, Volokitin AI, Tosatti E. On the nature of surface roughness with application to contact mechanics, sealing, rubber friction and adhesion. J. Phys. Cond. Matter 17, R1–R62 (2005)

[10] Pastewka L, Robbins MO. Contact between rough surfaces and a criterion for macroscopic adhesion. Proc. Nat. Acad. Sci. USA 111, 3298–3303 (2014)

[11] Yastrebov VA, Anciaux G, Molinari JF. From infinitesimal to full contact between rough surfaces: Evolution of the contact area. Int. J. Sol. Struct. 52, 83–102 (2015)

[12] Ben-David O, Rubinstein SM, Fineberg J. Slip-stick and the evolution of frictional strength. Nature 463, 76–79 (2010)

[13] Baumberger T, Caroli C. Solid friction from stick–slip down to pinning and aging. Adv. Phys. 55, 279–348 (2006)

[14] Zeroukhi Y, Napieralska-Juszczak E, Vega G, Komeza K, Morganti F, Wiak S. Dependence of the Contact Resistance on the Design of Stranded Conductors. Sensors 14, 13925–13942 (2014)

[15] Arrazat B, Duvivier PY, Mandrillon V, Inal K. Discrete Analysis of Gold Surface Asperities Deformation under Spherical Nano-Indentation towards Electrical Contact Resistance Calculation. IEEE 57th Holm Conference on Electrical Contacts, 1–8 (2011)

[16] Tekaya A. Influence de la dimensionnalité et de la complexité d'un réseau sous compression mécanique sur les transports électrique et thermique dans les milieux granulaires métalliques - De l'interface individuelle aux propriétés collectives, Doctoral Thesis, Université de Picardie Jules Verne (2012)

[17] Holm R. Electric Contacts - Theory and Applications, Springer (1967)

[18] Tabor D. The Hardness of metal. Clarendon Press, Oxford (1951)

[19] Foy N. Modélisation et simulation multi-physique des interfaces multi-contacts métal/métal. Doctoral Thesis, Université de Picardie Jules Verne (2017)

[20] Jonckheere B, Bouzerar R, Bourny V, Bausseron T, Foy N, Durand-Drouhin O, Le Marrec F, Chevallier E. Assessment of the real contact area of a multi-contact interface from electrical measurements. 23ème Congrès Français de Mécanique (2017)

[21] Courtney-Pratt JS, Eisner E. The effect of a tangential force on the contact of metallic bodies. Proceedings of the Royal Society of London Series A Math. and Phys. Sciences 238 (1957)

[22] Tekaya A, Bouzerar R, Bourny V, Tekaya I. Electron tunneling in metallic beads systems and slow electric relaxation. World of Engineering, Vol. 8, n°2 (2011)

[23] Tekaya A, Bouzerar R, Bourny V. Influence of surface topology on the electrical response of many bead assemblies. AIP Advances, 2, 032108 (2012)

[24] Rabinowicz E. The Nature of the Static and Kinetic Coefficients of Friction. Journal of Applied Physics, 22, 1373 (1951)

[25] Prevost A, Scheibert J, Debrégeas G. Probing the micromechanics of a multi-contact interface at the onset of frictional sliding. Eur. Phys. Journal E, 36 17 (2013)

[26] Sahli R, Pallares G, Ducottet C, Ben Ali IE, Al Akhrass S, Guibert M, Scheibert, J. Evolution of real contact area under shear and the value of static friction of soft materials. PNAS 115, 471-476 (2018)

[27] Sahli R, Pallares G, Papangelo A, Ciavarella M, Ducottet C, Ponthus N, Scheibert J. Shear-Induced Anisotropy in Rough Elastomer Contact. Phys. Rev. Letters, 122, 214301 (2019)

[28] Papangelo A, Scheibert J, Sahli R, Pallares G, Ciavarella M. Shear-induced contact area anisotropy explained by a fracture mechanics model. Phys. Rev. E, 99, 053005 (2019)

[29] Mergel JC, Sahli R, Scheibert J, Sauer RA. Continuum contact models for coupled adhesion and friction. The Journal of Adhesion, 95:12, 1101-1133 (2019)

[30] Brizmer V, Kligerman Y, Etsion I. A model for junction growth of a spherical contact under full stick condition. J. Tribology, 129, 783–790 (2007)

[31] Degrandi-Contraires E, Poulard C, Restagno F, Léger L. Sliding friction at soft micro-patterned elastomer interfaces. Faraday Discuss, 156, 255–265 (2012)

[32] Savkoor AR, Briggs GAD. The effect of tangential force on the contact of elastic solids in adhesion. Proc. R. Soc. London A Math. Phys. Sci., 356, 103–114 (1977)

[33] Varenberg M, Gorb S. Shearing of fibrillar adhesive microstructure: Friction and shear-related changes in pull-off force. J. R. Soc. Interface, 4, 721–725 (2007)

[34] Waters JF, Guduru PR. Mode-mixity-dependent adhesive contact of a sphere on a plane surface. Proc. R. Soc. A, 466, 1303–1325 (2009)

[35] Bourny V, Fortin J, Capitaine T, Lorthois A, Da Ros V. “Monitoring the quality of a Communication channel supported by a sliding contact”. Patent No. US20160142162 (US9917664B2).

[36] Puille C, Durand-Drouhin O, Le Marrec F, Bouzerar R, Bourny V, Lejeune M, Fortin J, Cantaluppi-Harlé A, Andasmas M. “Surveillance de l’état d’un dispositive de garniture mécanique”, Patente N0. FR3065286A1.

[37] Bourny V, Bouzerar R, Capitaine T, Fortin J, Lorthois A. “Surveillance de l'état d'un dispositif de roulement”, Patent No. FR3016041A1.

FIGURES

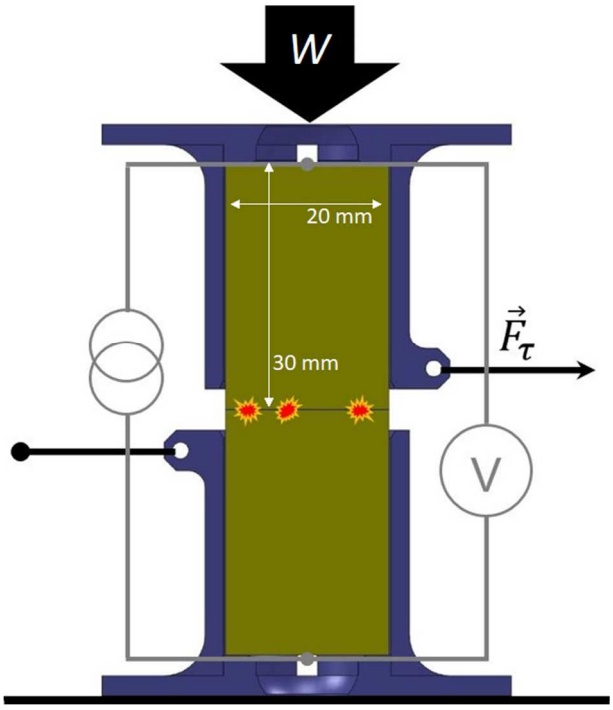

Fig.1. Experimental apparatus.

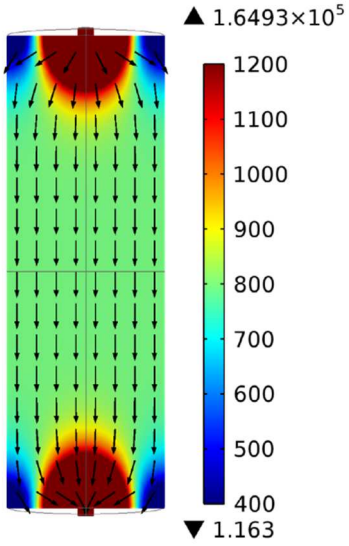

Fig.2. Current distribution into the contacting cylinders (I=250mA, unit in A/m²).

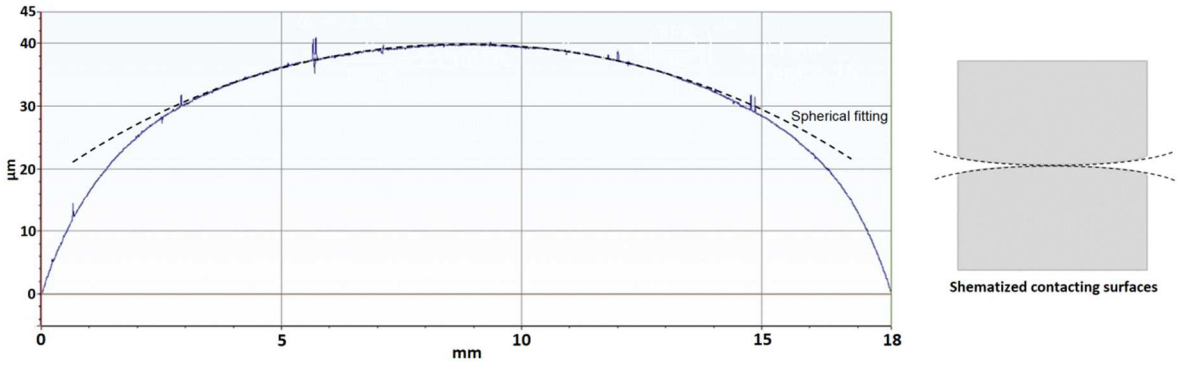

Fig.3a. Global shape of contact surface.

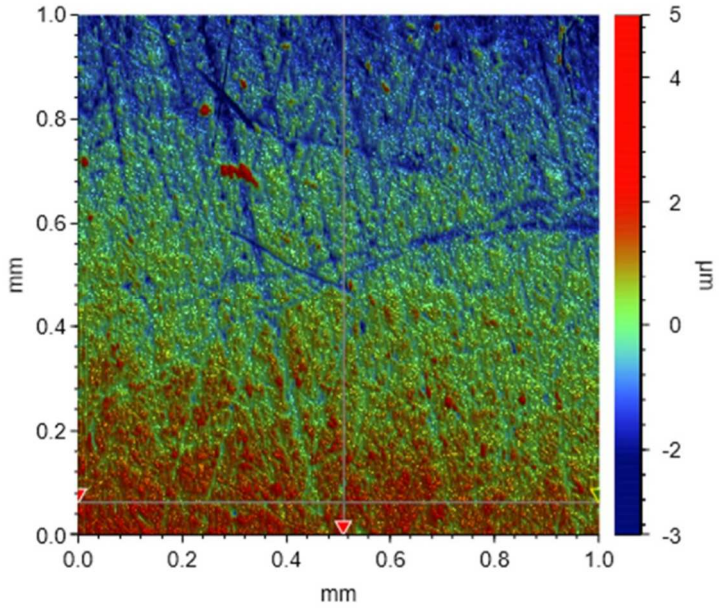

Fig3b. Map of a part of contact surface.

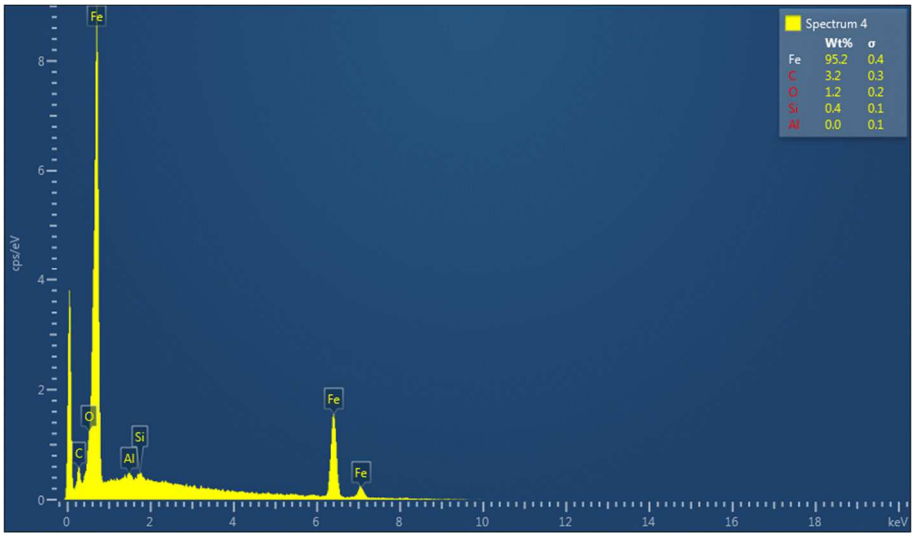

Fig.4. Chemical analysis of contact surface.

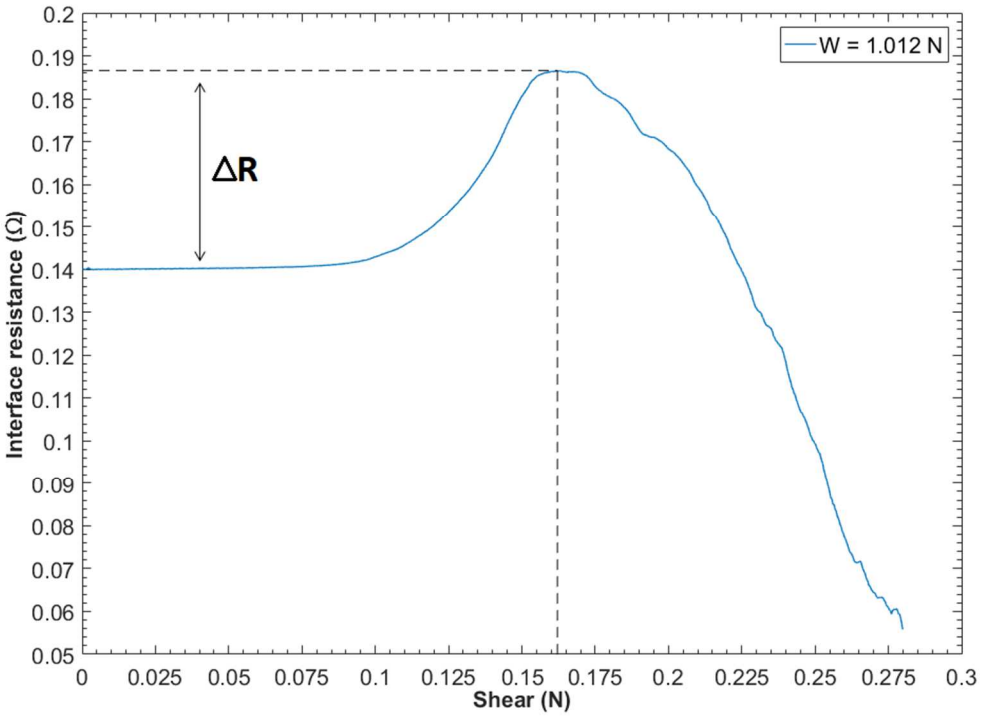

Fig.5. Evolution of the interface resistance versus the applied shear under a normal load around 1N.

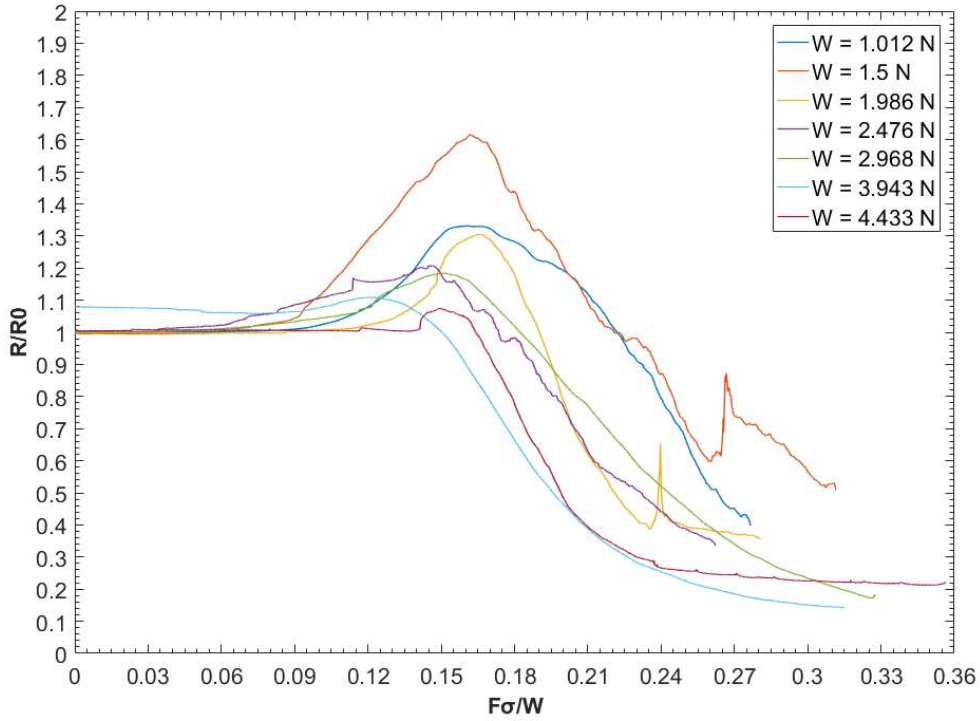

Fig.6. Evolution of R/R_0 *vs.* F_σ/W under different normal load.

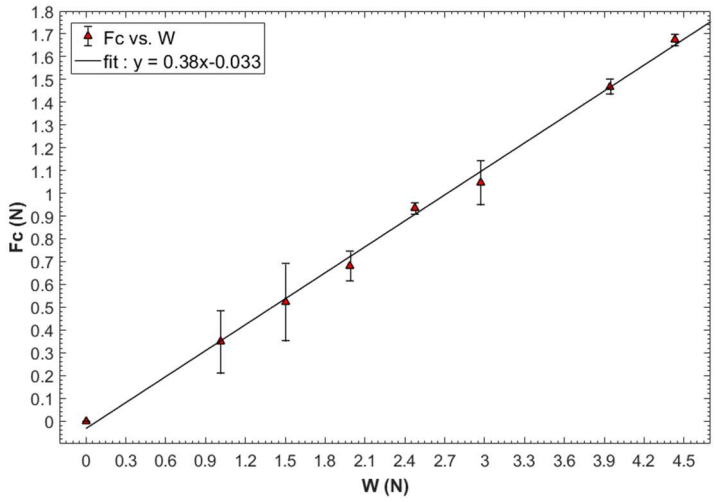

Fig.7. Linear fitting of the critical value of shear (contact breaking) versus the applied normal load. The static friction coefficient μ_S is estimated around 0.38.

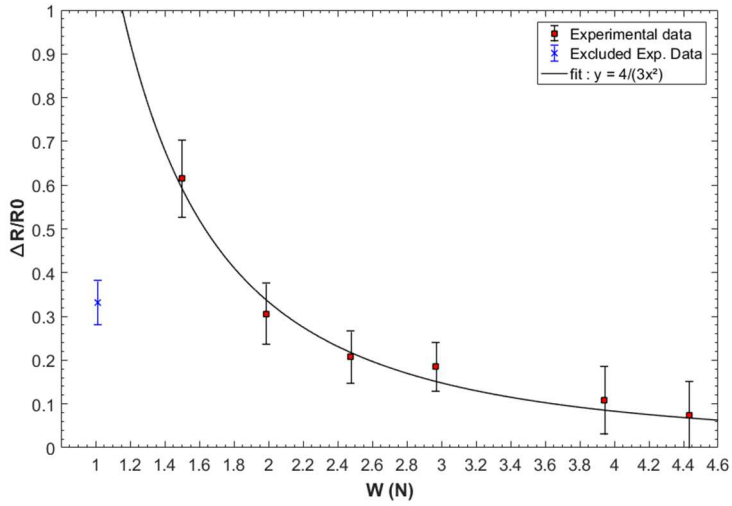

Fig.8. Evolution of $\Delta R/R_0$ versus the normal load.

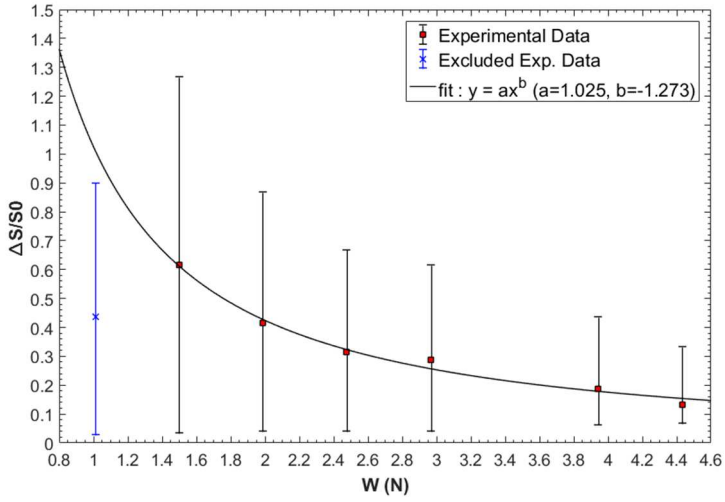

Fig.9. Evolution of $\Delta S/S_0$ versus the normal load.

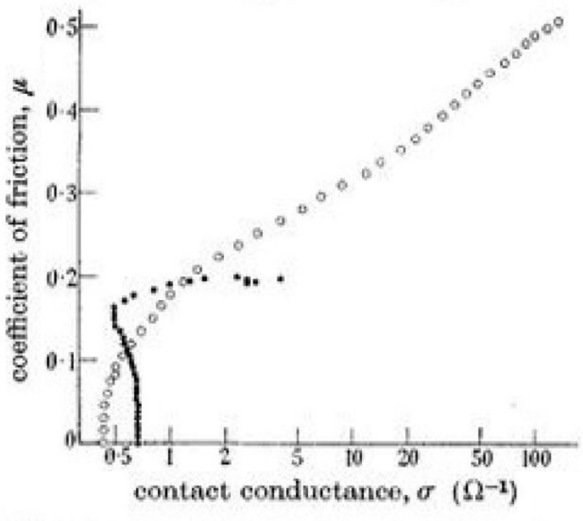

Fig.10. Friction coefficient vs. contact conductance from [21]: ○ dry contact, ● lubricated contact.

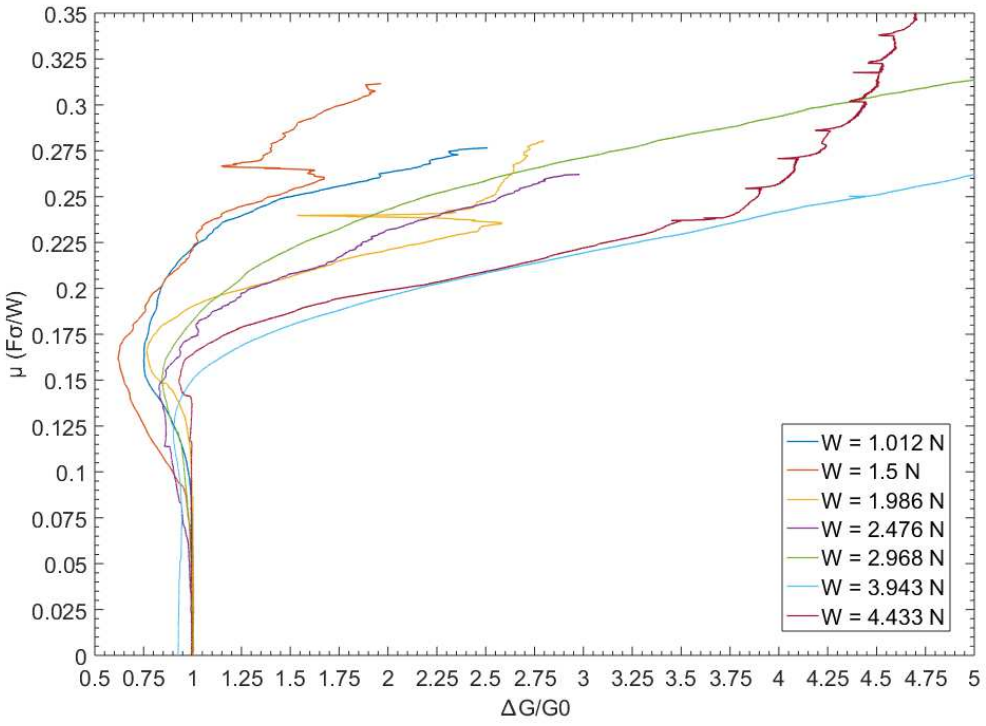

Fig.11. Friction coefficient vs. normalized contact conductance, for different normal loads. The value of $\Delta G/G_0$ is directly deduced from $\Delta R/R_0$ since $G = 1/R$.